

# Online Research @ Cardiff

This is an Open Access document downloaded from ORCA, Cardiff University's institutional repository: <https://orca.cardiff.ac.uk/id/eprint/129640/>

This is the author's version of a work that was submitted to / accepted for publication.

Citation for final published version:

Tasseroul, Jonathan, Lorenzo-Garcia, Maria Mercedes, Dosso, Jacopo ORCID: <https://orcid.org/0000-0003-4173-3430>, Simon, Francois, Velari, Simone, De Vita, Alessandro, Tecilla, Paolo and Bonifazi, Davide ORCID: <https://orcid.org/0000-0001-5717-0121> 2020. Probing peripheral H-bonding functionalities in BN-doped polycyclic aromatic hydrocarbons. Journal of Organic Chemistry 85 (5) , pp. 3454-3464. 10.1021/acs.joc.9b03202 file

Publishers page: <http://dx.doi.org/10.1021/acs.joc.9b03202>  
<<http://dx.doi.org/10.1021/acs.joc.9b03202>>

Please note:

Changes made as a result of publishing processes such as copy-editing, formatting and page numbers may not be reflected in this version. For the definitive version of this publication, please refer to the published source. You are advised to consult the publisher's version if you wish to cite this paper.

This version is being made available in accordance with publisher policies.

See

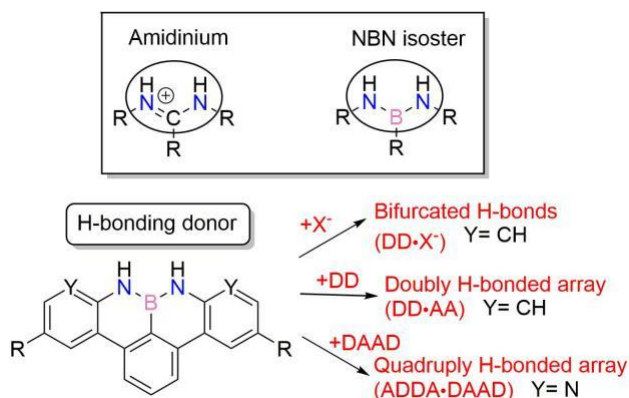
<http://orca.cf.ac.uk/policies.html> for usage policies. Copyright and moral rights for publications made available in ORCA are retained by the copyright holders.



# Probing peripheral H-bonding functionalities in BN-doped polycyclic aromatic hydrocarbons.

Jonathan Tasseroul<sup>†</sup>, M. Mercedes Lorenzo-Garcia<sup>§</sup>, Jacopo Dosso<sup>§</sup>, François Simon<sup>†</sup>, Simone Velari,<sup>‡</sup> Alessandro De Vita<sup>#,‡</sup>, Paolo Tecilla<sup>||</sup> and Davide Bonifazi<sup>†,§,\*</sup>

<sup>†</sup>Department of Chemistry, University of Namur (UNamur), Rue de Bruxelles 61, B-5000, Namur, Belgium; <sup>§</sup>School of Chemistry, Cardiff University, Park Place, Main Building, CF10 3AT, Cardiff, United Kingdom, [bonifazid@cardiff.ac.uk](mailto:bonifazid@cardiff.ac.uk); <sup>||</sup>Department of Chemical and Pharmaceutical Science, University of Trieste, Piazzale Europa 1, 34127 Trieste, Italy; <sup>‡</sup>Department of Engineering and Architecture, University of Trieste, Piazzale Europa 1, 34127 Trieste, Italy; <sup>#</sup>Department of Physics, King's College London, Strand, London WC2R 2LS, United Kingdom



**ABSTRACT:** The replacement of carbon atoms at the zig-zag periphery of a benzo[fg]tetracenyl derivative with an NBN atomic triad allows the formation of heteroatom-doped PAHs isosteres, which expose BN mimics of the amidic NH functions. Their ability to form H-bonded complexes has never been touched so far. Herein we report the first solution recognition studies of peripherally NBN-doped PAHs to form doubly H-bonded DD•AA and ADDA•DAAD-type complexes with suitable complementary H-bonding acceptor partners. The first determination of the  $K_a$  in solution showed that the 1:1 association strength is around  $27 \pm 1 \text{ M}^{-1}$  for the DD•AA complexes in  $\text{C}_6\text{D}_6$ , whereas it rises to  $1820 \pm 130 \text{ M}^{-1}$  for the ADDA•DAAD array in  $\text{CDCl}_3$ . Given the interest of BN-doped polyaromatic hydrocarbons in supramolecular and materials chemistry, it is expected that these findings will open new possibilities to design novel materials, where the H-bonding properties of peripheral NH hydrogens could serve as anchors to tailor the organizational properties of PAHs.

## INTRODUCTION

Following the vigorous synthetic developments of polycyclic aromatic hydrocarbons (PAHs),<sup>1</sup> the substitution (*i.e.*, doping) of  $\text{sp}^2$ -carbon atoms with isoelectronic and isostructural BN couples is re-emerging as a versatile approach to tune the optoelectronic properties of these materials.<sup>2–7</sup> In particular, borazines<sup>8,9</sup> and BN-doped PAHs (*e.g.*, azaborines,<sup>10,11</sup> borazapyrenes,<sup>12,13</sup> borazaphenanthrenes<sup>12,14</sup> borazanaphthalenes,<sup>15,16</sup> borazaanthracene<sup>17,18</sup> and borazaperylene<sup>19</sup>) are now increasingly attracting the attention of the physical and chemical community for their use in a broad spectrum of optoelectronic applications.<sup>20–22</sup> When used to decorate a periphery, non-substituted BN couples terminate with NH functions that, being more acidic than the CH analogues, could engage into H-bonding interactions as observed with boronic acids.<sup>23</sup> For instance, Liu and co-workers showed in a seminal report that 1,2-dihydro-1,2-azaborine can act as an H-bonding donor in the solid state and engage into a H-bond with the  $\text{C}=\text{O}$

group of a glutamine side chain in a T4 lysozyme.<sup>24,25</sup> However, to the best of our knowledge, no examples of studies describing and measuring the strength of H-bonding interactions in solutions with BN-doped peripheries have been reported to date.

While attempting different synthetic strategies to prepare hexabenzoborazinocoronene,<sup>26</sup> we prepared the NBN-doped isostere of a benzo[fg]tetracenyl anion (Figure 1). Derivatives of the NBN-doped isostere were firstly prepared independently by the groups of Hatekeyama<sup>27</sup> and Feng<sup>28</sup>. When looking at the NBN-doped zig-zag periphery, one notice that the unsubstituted HNBNH array is a neutral H-bonding mimic of an amidinium moiety, known to establish doubly H-bonded DD-AA-type arrays. DFT calculations (see SI for the details) on the all-carbon analogue (CCC) and its NBN-doped isostere suggest that the HOMO and LUMO distributions are very similar on both molecules, with the NBN atomic triad negligibly contributing to the LUMO (Figure S39) in line with the data reported by Hatekeyama<sup>27</sup> and Feng<sup>28</sup>. Remarkably, the lack of contribution from the B atom is observable for the LUMO orbital, advocating a tenuous electrophilic character of the B atom center (Figure S39). On the other hand, a significant contribution from the N atoms is noticeable for the HOMOs with the involvement of the B atom remaining negligible. As expected, the NBN-doping results in a low-lying HOMO, the latter contributing significantly to the increase of the HOMO-LUMO gap with respect to the 22- $e^-$  all-carbon benzo[fg]tetracenyl derivative (Figure S39).

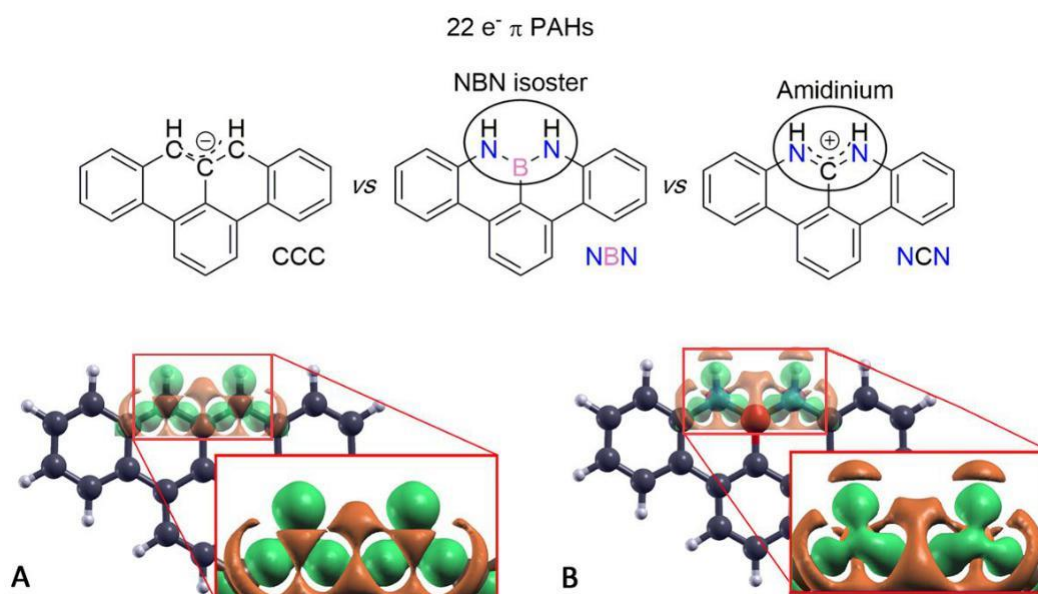


**Figure 1.** Neutral NBN isosteres of polycyclic aromatic benzo[fg]tetracenyl anions. Charge density distribution for the A) CCC and B) NBN-doped scaffold as calculated at the DFT theory level using the ab initio pseudopotential plane-wave method as implemented in the PWSCF code of the Quantum ESPRESSO distribution (electron density accumulation is depicted in green, depletion in orange).

DFT calculations also reveal a peculiar distribution of the electron density around the NH group as shown by the charge density transfer plots (calculated as  $\rho_{\text{mol}} - \Sigma \rho_{\text{atom}}$ , where  $\rho_{\text{mol}}$  is the charge density of the molecule and  $\rho_{\text{atom}}$  the density of the single atoms) in Figure 1b. The decreasing of charge density for the aminic H atoms is induced by the presence of the electronegative N atoms and is clearly visible in the NBN-doped molecule while it is absent for the iso-positional H atoms of the CCC analogue (Figure 1a). As observed by Liu and co-workers,<sup>29</sup> this suggests that the NH groups are acidic, and thus possibly enabling the formation of doubly H-bonding interactions in the presence of a suitable H-bond acceptor. ESP calculations showed that molecule **1** displays a great charge depletion on the NH groups and B atoms, whereas the carbocyclic backbone remains slightly negatively charged (Figure 2). These results are consistent with the calculated electron density properties, further suggesting that this peculiar NBN motif can be considered as a neutral isostere of substituted amidinium cations, known to behave as a H-bonding DD-type array.<sup>30</sup>

This prompted us to study the H-bonding abilities of the NBN-doped moiety towards suitable complementary H-bonding acceptors, such as fluoride ions and complementary AA-type H-bonding guests. Thus, we synthesized NBN-doped benzo[fg]tetracenyl derivatives **1** and **2**, which should undergo formation of bifurcated and doubly H-bonds arrays with  $F^-$  ions and 1,8-naphthyridine, respectively (Figure 3). When comparing the H-bonding NBN-doped array with that of the amidinium, one can hardly fail to notice that the amidinium is expected to present the strongest association due to the presence of charge-dipole interactions. Building on this hypothesis, we conjectured that BN-doped scaffold **3**, in which the lateral fused benzene rings have been substituted by two pyridines, should behave as an ADDA-type H-bonding motif (Figure 3). In the presence of a suitable complementary H-bonding DAAD-type partner, molecule **3** is expected to form quadruply H-bonded ADDA•DAAD arrays featuring higher association constants than those hypothesized for DD•AA complexes. For this reason, we also prepared receptor **3** and studied its H-bonding recognition properties in the presence of diacetyl-2,7-diaminonaphthyridine (Figure 3). All molecules were equipped with either 2-phenylethyl chains (**1**) or mesitylene moieties (**2** and **3**) to increase solubility in organic solvents.

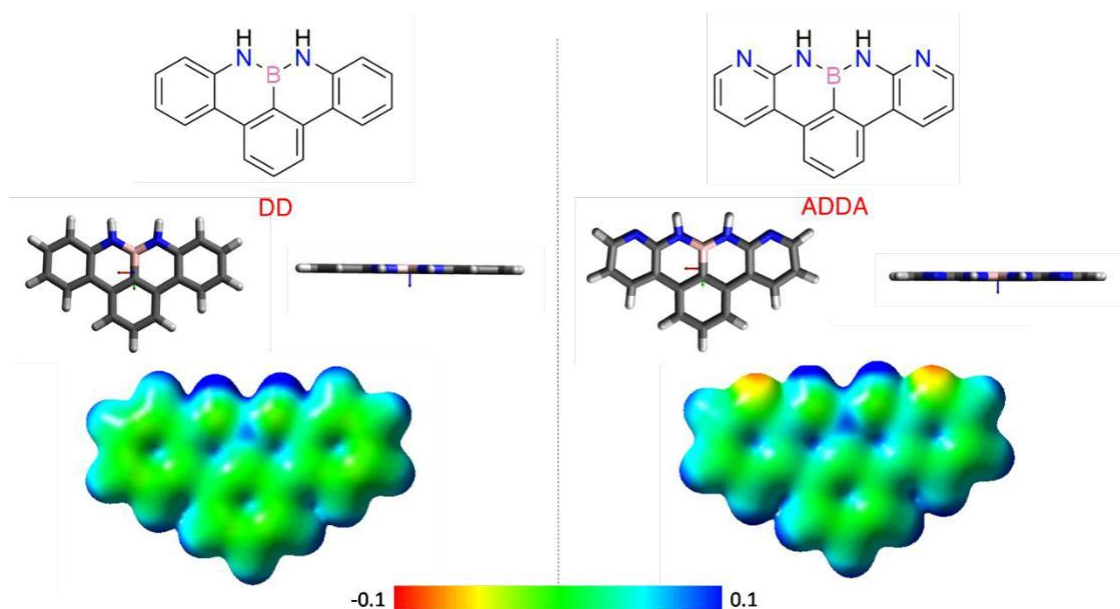


**Figure 2.** DFT calculations at the B<sub>3</sub>LYP/6-311G\*\* level of theory of the structural and ESP properties of the NBN-doped benzo[fg]tetracenyl derivatives exposing H-bonding recognition DD- (left) and ADDA-type (right) arrays.

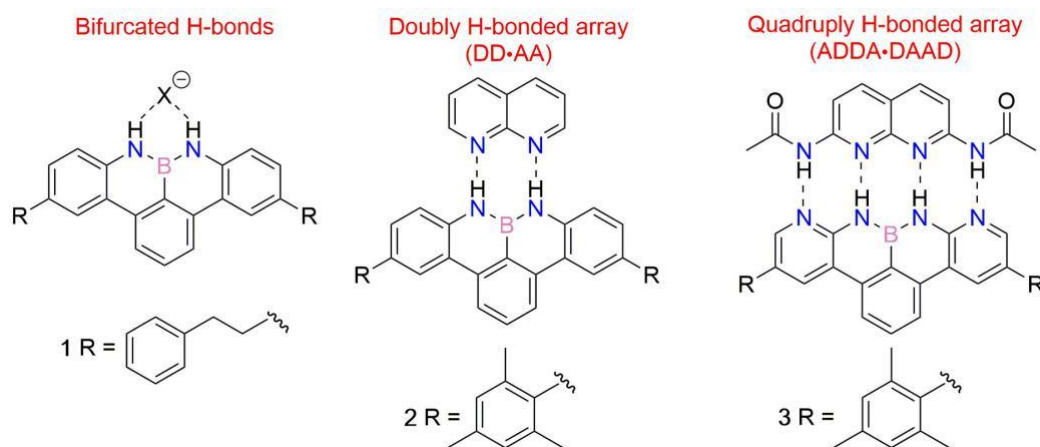
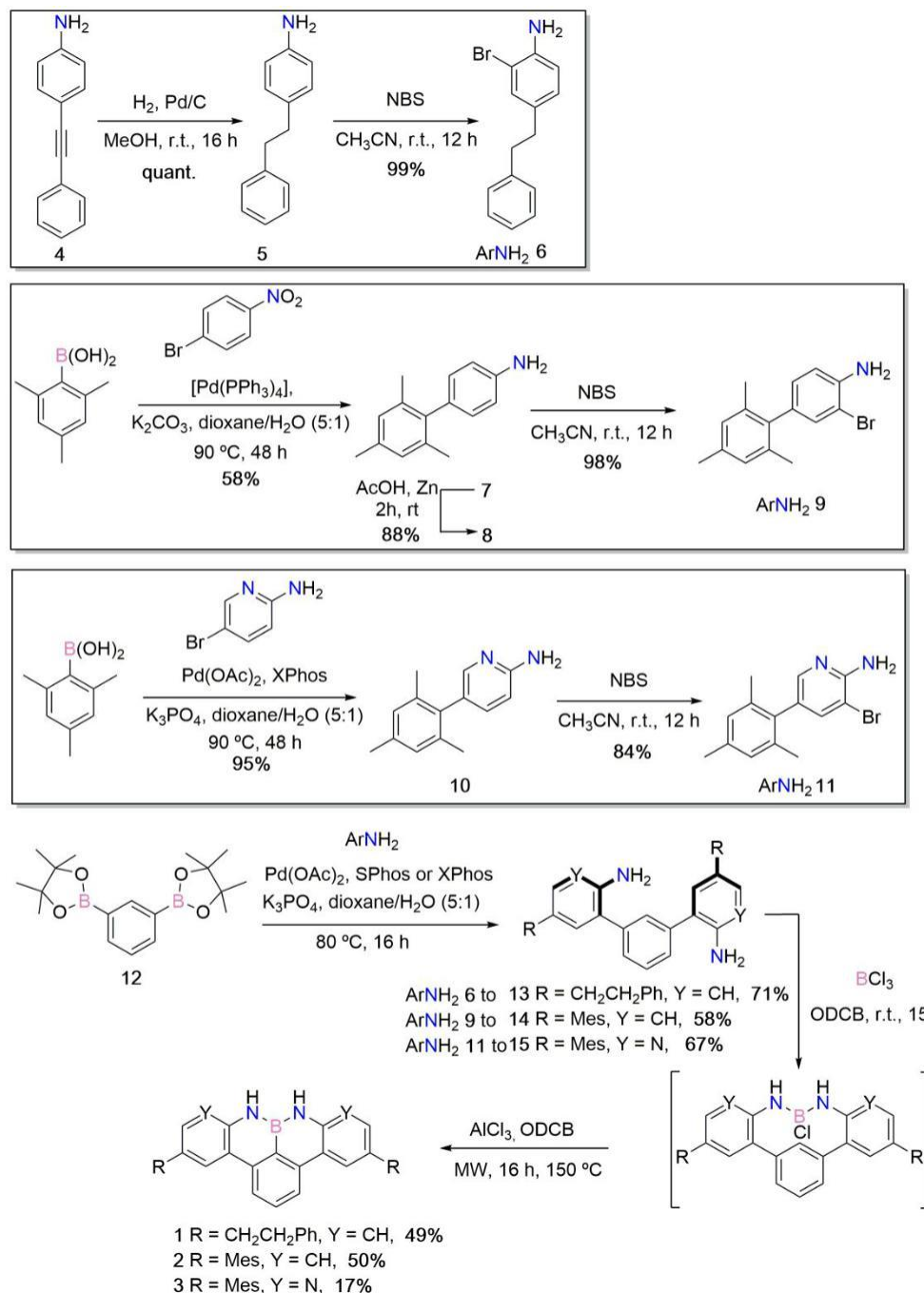


**Figure 3.** H-bonded arrays and recognition modes studied in this work.



**Synthesis and structural characterization.** We synthesized the NBN core starting from the relevant aniline bearing the chosen solubilizing group instead of performing a post-synthetic functionalization of the NBN-doped benzo[fg]tetracenyle. This choice allows to obtain differently substituted HNBNH derivatives without the need of protecting groups for the aminic moieties. Moreover, to increase the synthetic versatility of the route, we decided to explore cyclisation conditions for the preparation of the NBN-doped PAHs that start from an unsubstituted polyphenylene scaffold. The syntheses of the three aniline precursors are reported in the insets of Scheme 1. The first step of the synthesis of **6** is the Pd/Cu-catalyzed Sonogashira cross-coupling of *para*-iodoaniline with phenylacetylene, yielding phenylacetylene-aniline **4**.<sup>31</sup>



**Scheme 1.** Synthetic routes towards aniline precursors **6**, **9**, and **11** (above) and NBN-doped scaffolds **1**, **2**, and **3** (below).

Its reduction with Pd/C in MeOH afforded phenethylaniline **5**, which was transformed into 3-bromoaniline **6** in quantitative yield by bromination reaction with NBS at rt. Similarly, anilines **9** and **11** were obtained starting from Suzuki-Miyaura cross-coupling reaction between 2,4,6-trimethylphenylboronic acid and either *p*-bromonitrobenzene or 2-amino-5-bromopyridine to give intermediates **7** and **10** in 58% and 95% yield, respectively. Nitro-derivative **7** was reduced with AcOH/Zn (88% yield) and the resulting amine brominated with NBS at rt to give substituted aniline **9** in quantitative yield. Analogously, bromination of **10** with NBS gave final aniline **11** in excellent yield (84 %). The aniline precursors were then cross-coupled through Suzuki-Miyaura reaction with phenylene bisboronate **12** in the presence of Pd(OAc)<sub>2</sub>, SPhos (or XPhos) and K<sub>3</sub>PO<sub>4</sub>, to give bis-aniline intermediates **13**, **14** and **15** in 71%, 58%, 67% yield, respectively (Scheme 1). Our synthetic studies to prepare NBN-doped PAH by cyclization on an un-substituted aromatic scaffold were commenced using bis-aniline **13** as substrate. Building on a general borylation procedure following modified versions of the approaches previously described by Dewar and later by Hatakeyama,<sup>20</sup> in a first attempt, we performed an intramolecular Friedel-Crafts cyclization reaction starting from the amino-BCl<sub>3</sub> intermediate in the presence of AlCl<sub>3</sub> in ODCB at 150°C. Unfortunately, these conditions were unsuccessful, and no conversion was observed. Similarly, deprotonation of bis-aniline **13** with two equivalents of *n*-BuLi at -84°C followed by the addition of BCl<sub>3</sub> at rt and Friedel-Crafts cyclization reaction did not lead to any transformation, and only starting material was recovered. On the other hand, changing the conventional oil-bath heating to a microwave irradiation, 100% conversion was observed, affording desired molecule **1** in 49% yield after purification. As expected, no reaction took place in the absence of AlCl<sub>3</sub>, even when two equivalents of BCl<sub>3</sub> were used. Subjecting amino-precursors **14** and **15** to the same procedure, compounds **2** and **3** were obtained in 50% and 17% yield, respectively. All three compounds exhibit an excellent chemical and thermal stability. The structure of all intermediates and products were unambiguously identified by HR-MS through the detection of the peak corresponding to the molecular mass of the ion (M<sup>+</sup>) and by <sup>1</sup>H-, <sup>13</sup>C- and <sup>11</sup>B-NMR, and IR spectroscopies (see SI, Figures S1-S29). Exemplary <sup>1</sup>H-NMR spectra of NBN-doped derivatives **1** in THF-*d*<sub>8</sub> and **3** in CDCl<sub>3</sub> are reported in Figure 4. Proton resonances *H*(*a*), *H*(*b*), and *H*(*c*) of structure **1** appear distinctively as triplet at 7.67 ppm, doublet at 8.11 ppm, and broad singlet at 8.05 ppm, respectively. These three signals are highly deshielded, confirming the polycyclic aromatic character of the structure. The signal of the NH protons appears as broad singlet centered at 7.31 ppm. Similarly, for molecule **3** the *H*(*a*) and *H*(*b*) resonances appear at 8.31 ppm and 8.15 ppm, respectively. The *H*(*c*)- and *H*(*b*)- peaks are visible as doublet and triplet at 8.11 ppm and 7.79 ppm followed by the resonances of the NH(*f*) protons at 7.36 ppm. The <sup>11</sup>B-NMR spectrum of **1** (Figure 4, inset) displays a broad peak centered at 26.4 ppm, the chemical shift of which is in agreement with that reported for similar NBN triads.<sup>32,33</sup>

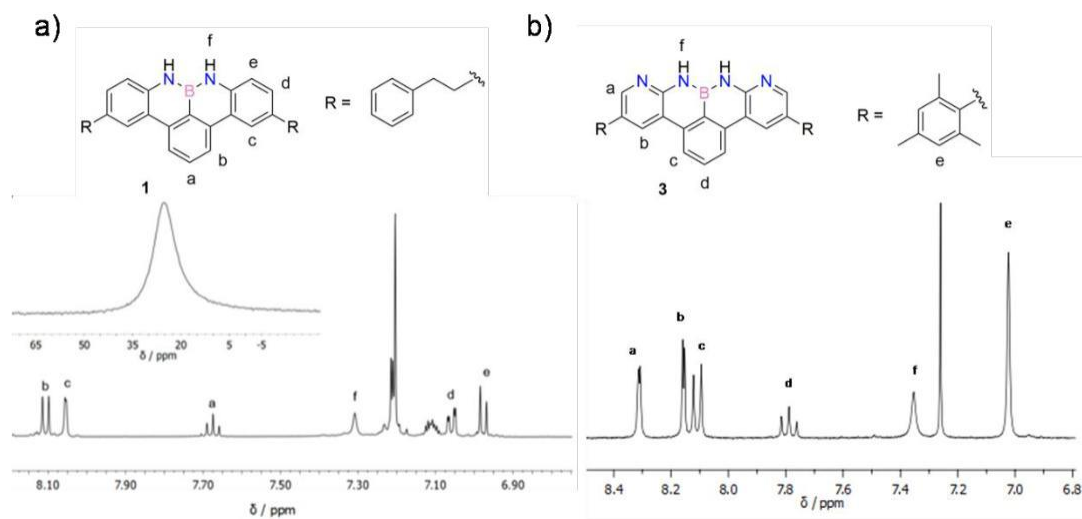


**Figure 4.** a) <sup>1</sup>H- and <sup>11</sup>B-NMR spectra for **1** in THF-*d*<sub>8</sub> at 298 K and b) <sup>1</sup>H-NMR spectra of **3** in CDCl<sub>3</sub>.

The photophysical properties of molecule **1** were investigated in THF solutions (see SI, Figure S30). Emission measurements display a blue fluorescence with a  $\Phi$  value of 21% (reference anthracene,  $\text{exc} = 372 \text{ nm}$ ), with the spectrum displaying a mirror image of the two lowest-energy absorption bands. The Stokes shift was as small as 27 nm, indicating a good rigidity of the structure, as expected for a fully fused PAH. The optical gap ( $E_{00}$ ) of **1**, deduced from the emission highest-energy peak, has been calculated to be 3.22 eV. Cyclic voltammetry (Figures S33) of **1** in THF shows a clear reversible mono electronic oxidative wave at 0.4 V (vs.  $\text{Fc}/\text{Fc}^+$ ). This allowed us to calculate the HOMO and LUMO energy levels, which revealed to be -5.51 eV and -2.29 eV, respectively (the LUMO energy level was estimated from  $E_{00}$ ). Overall, these data are in agreement with those reported for the unsubstituted NBN derivative in  $\text{CH}_2\text{Cl}_2$  and predicted by DFT Calculations (Figure S39).<sup>27,28</sup>

**Titration experiments and determination of the H-bonding recognition abilities.** We started with the  $\text{F}^-$  ions as probes to study the recognition properties of molecule **1** toward bifurcated H-bonded complexes. The interaction was studied in THF solutions through spectroscopic UV-vis absorption titration experiments (Figure 5). In particular, a standard solution of TBAF was added stepwise to a  $4.43 \times 10^{-5} \text{ M}$  solution of **1** at 298 K and the steady-state UV-vis absorption spectra taken (Figure 5, above). Upon addition of increasing concentration of TBAF, the intensity of the band centered at 360 nm decreases and a new transition develops at 390 nm. Similar red shift of the lowest-energy band had been previously observed when fluoride ions interact with other DD-type H-bonding systems, like urea derivatives.<sup>34,35</sup> Notably, no marked color changes were observed during the titration experiments, suggesting that molecule **1** likely does not undergo deprotonation (see also Figures S31-32 for the color change and UV-vis spectra of the mono- and bis-anionic species obtained upon addition of one and two equivalents of *sec*-BuLi). Complementary  $^1\text{H}$ -NMR titrations with a  $1 \times 10^{-3} \text{ M}$  solution of **1** (Figure S38) showed a fast equilibrium, triggering a progressive downfield shift of the NH protons from 7.30 to 10.60 ppm upon the incremental addition of TBAF. Together with the  $H(f)$  resonances, also the signals of the aromatic peri-protons  $H(e)$  experience a progressive deshielding upon stepwise addition of TBAF confirming the frontal arrangement of the H-bonded complex. However, the signal of the NH protons in presence of up to 2 equivalents of TBAF is rather broad, almost no detectable, and in the presence of larger excess of fluoride remains broad and non-symmetric. This hampered a quantitative determination of the association constant ( $K_a$ ) in THF. Moreover, it is likely that the equilibrium is made more complex by concurrent additional equilibria, such as the formation of the corresponding bialide specie ( $\text{HF}_2^-$ ), which is known to take place in organic solvents.<sup>36</sup>

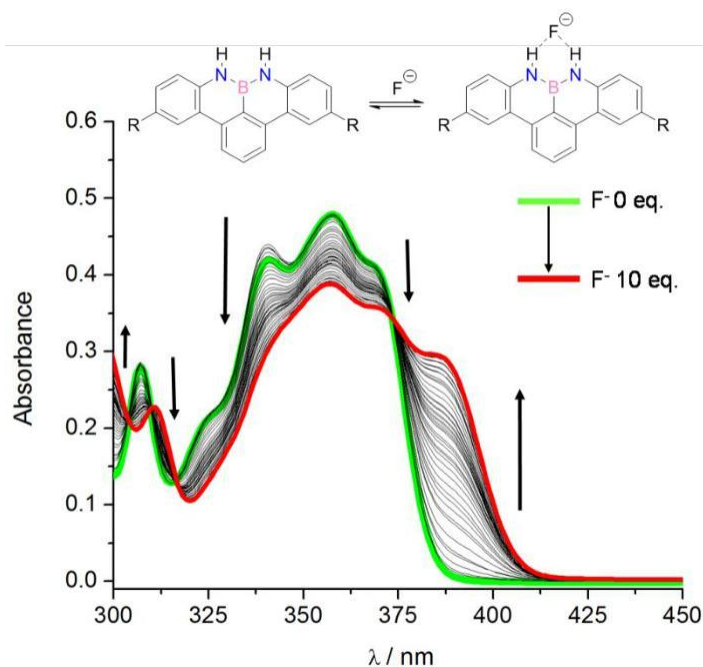


**Figure 5.** UV-Vis titrations of **1** ( $c_0 = 4.43 \times 10^{-5} \text{ M}$ ) in THF at 298 K with TBAF.

Complementary  $^{11}\text{B}$ -NMR studies showed that the chemical shift of the B resonance is unaffected by the incremental addition of TBAF (Figure S38), thus excluding the presence of any competitive interactions established between the B center and the  $\text{F}^-$  ions further confirming the formation of H-bonded complex  $\mathbf{1}\cdot\text{F}^-$  in solution. This is in line with the theoretical finding, which revealed an elusive contribution of the B atom to the LUMO orbital of  $\mathbf{1}$ .

To further investigate H-bonding properties of the NBN-doped PAHs, we studied the binding of molecules  $\mathbf{2}$  and  $\mathbf{3}$  with 1,8-naphthyridine (**NAP**) and diacteyl-2,7-diaminonaphthyridine (**DAN**).<sup>37</sup> While **NAP** should form doubly H-bonded DD•AA arrays with  $\mathbf{2}$  and  $\mathbf{3}$ , **DAN** should undergo quadruply ADDA•DAAD complexes with  $\mathbf{3}$  (Figure 3). Addition of increasing amount of **NAP** to an 8 mM solution of  $\mathbf{3}$  in  $\text{CD}_2\text{Cl}_2$  up to 2.5 equivalents led to minor linear downfield shift of the  $H(f)$  resonances, suggesting the formation of an H-bonded complex with a low  $K_a$  value (Figure S34). This was confirmed by changing the solvent to less polar and less competitive  $\text{C}_6\text{D}_6$ , in which the formation of H-bonds is favored (Figure 6).<sup>38</sup>

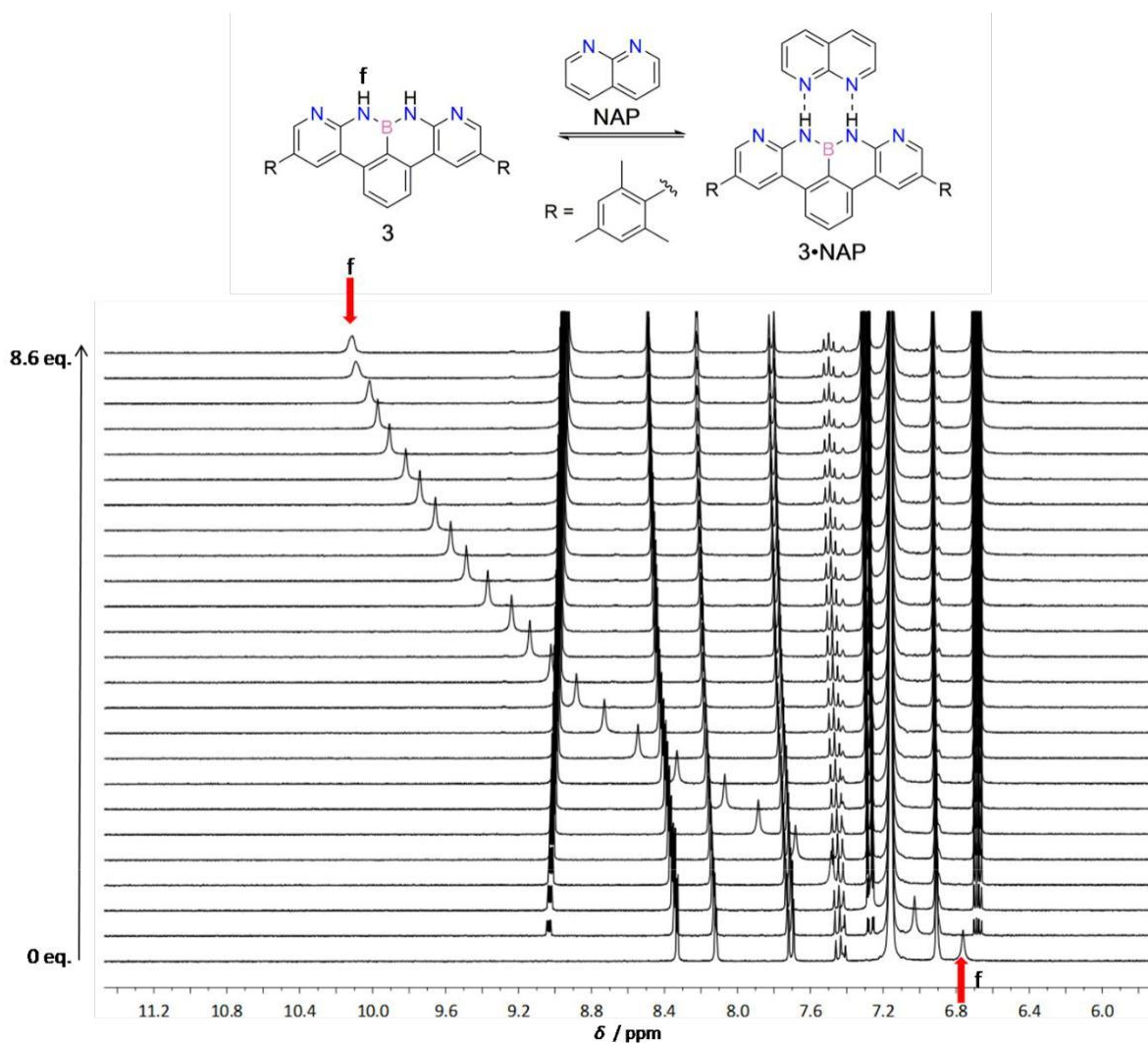


**Figure 6.**  $^1\text{H}$ -NMR (400 MHz) titration of  $\mathbf{3}$  ( $c_0 = 9.30 \times 10^{-3} \text{ M}$ ) with **NAP** in  $\text{C}_6\text{D}_6$  at 298 K.

Upon addition of increasing amount of **NAP** (up to 8.6 equivalents) to a  $9.30 \times 10^{-3} \text{ M}$  solution of  $\mathbf{3}$  in  $\text{C}_6\text{D}_6$ , a large downfield shift ( $> 3.3$  ppm) of the  $H(f)$  protons was observed typical of the formation of an H-bonded complex under a regime of fast equilibrium exchange (Figure 6). Together with the  $H(f)$  resonances, also the peaks of the proton resonances of the lateral pyridyl moieties revealed significant downfield shifts upon addition of **NAP**, confirming the frontal arrangement of the H-bonded DD•AA complex.



The same picture is obtained by titrating molecule **2** with **NAP** in  $C_6D_6$  (see Figure S36). Fitting the chemical shift values of the  $H(f)$  resonances from the titration experiments of **3** and **2** with **NAP** to a 1:1 binding isotherm with Dynafit,<sup>39</sup> gave  $K_a$  values of  $25 \pm 1 \text{ M}^{-1}$  and  $27 \pm 1 \text{ M}^{-1}$  for complexes **3**•**NAP** and **2**•**NAP**, respectively (Figures S35-36). Notably, these H-bonded DD•AA-type complexes show association strengths considerably lower than those observed with a series of aromatic boronic acids that, in their *syn-syn* conformation, showed 1:1 association in the range between 300 and 6900  $\text{M}^{-1}$ .<sup>23</sup> Further evidences of the ability of the NBN motif to undergo H-bonding recognition and form supramolecular complexes, came from the titration studies of molecule **3** with complementary DAAD-type **DAN** derivative. As **DAN** is almost insoluble in benzene, the titration was performed in the more polar and more competitive  $CDCl_3$  solvent. As shown in Figure 7, titration of a  $4.94 \times 10^{-3} \text{ M}$  solution of **3** with increasing amounts of **DAN**, up to 3.36 equivalents, resulted in a large downfield shift ( $> 3.3 \text{ ppm}$ ) of the  $H(f)$  resonances. This suggested the formation of a frontal H-bonded ADDA•DAAD complex. The calculated  $K_a$  value for the 1:1 complex **3**•**DAN** was found to be  $1820 \pm 130 \text{ M}^{-1}$  in  $CDCl_3$ , which is more than 70 times higher than that measured for the **3**•**NAP** in  $C_6D_6$ . JOB's analysis of the titration data confirmed the 1:1 stoichiometry of the quadruply H-bonded **3**•**DAN** complex (Figure S37).

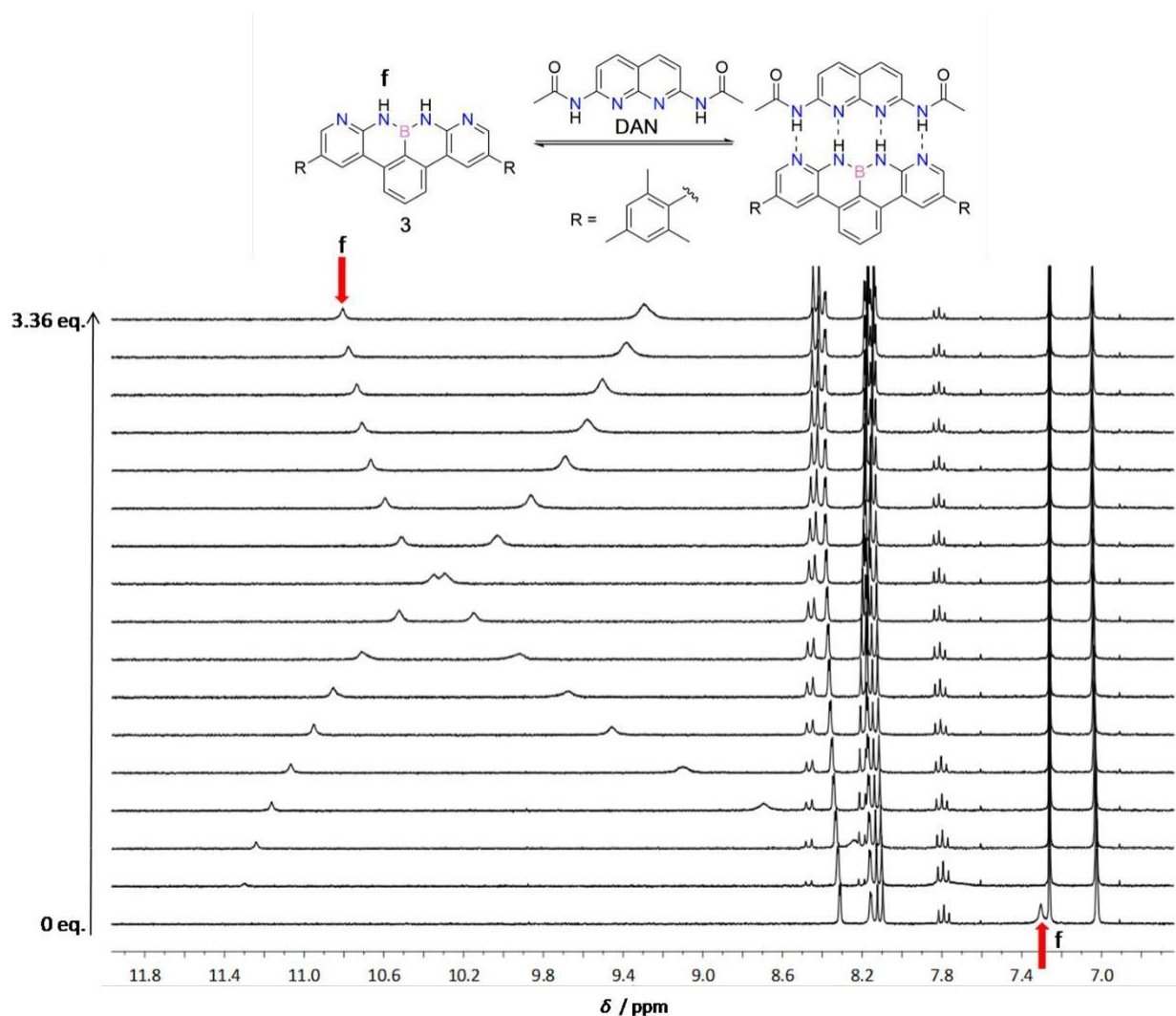


**Figure 7.**  $^1\text{H}$ -NMR (400 MHz) titration of receptor **3** ( $c_0 = 4.94 \times 10^{-3} \text{ M}$ ) with **DAN** in  $CDCl_3$  at 298 K.

Despite the numerous attempts, we could not grow suitable crystals for X-ray diffraction analysis of both the single components (**1**, **2** and **3**) and H-bonded complexes (**2**•**NAP**, **3**•**NAP** and **3**•**DAN**). Therefore, we turned our attention to NOESY experiments to confirm the structure of the hypothesized hydrogen-bonded complex. The  $^1\text{H}$ - $^1\text{H}$  NOESY spectrum of a  $7.0 \times 10^{-3} \text{ M}$  solution of **3**

in the presence of 1.1 eq. of **DAN** was recorded (Figure 8). From this analysis, one can easily discern a through space interaction (Figure 8a) between protons  $H(b)$  and  $H(g)$ , which allowed the unambiguous assignment of the resonances attributed to  $H(a)$  and  $H(b)$ . A clear peak assignment could not be made from  $^1\text{H}$ - $^1\text{H}$  COSY spectra (Figure S16). Interestingly, the through space interaction between protons  $H(i)$  of the Me groups of **DAN** and protons  $H(a)$  of **3** (Figure 8b) suggests that a close spatial proximity exist for these atoms, unambiguously confirming the structure of the proposed frontal H-bonding arrangement for complex **3**•**DAN**.

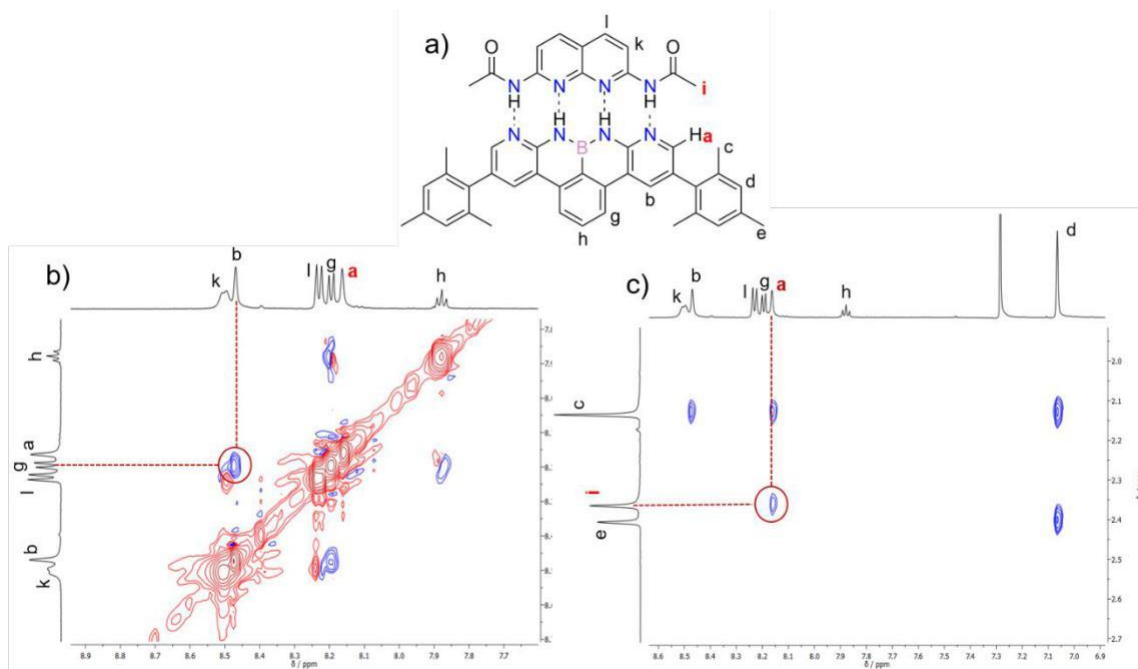


**Figure 8.** a) Arrangement of hydrogen bonded aggregates; 2D  $^1\text{H}$ -NOESY NMR (600 MHz) of receptor **3** ( $c_0 = 7.0 \times 10^{-3}$  M) with **DAN** in  $\text{CDCl}_3$  at 298 K; ratio of **3** to **DAN**: 1:1.1. b) detail of aromatic part with through space interaction between  $H(b)$  and  $H(g)$  highlighted; c) zoom on the through space interaction between  $H(a)$  and  $H(i)$ .

## CONCLUSIONS

In conclusion, in this paper we describe the synthesis of a family of NBN isosteres of a full-carbon benzo[fg]tetracenyl anion with improved solubility in different organic solvents. The NBN functional group could be inserted in a zig-zag topology allowing the planarization of the three aryl rings. DFT calculations of the charge density showed significant charge depletion at the NH protons, anticipating good H-bonding capabilities of this NBN functional group. This was for the first time demonstrated by spectroscopic titration of molecule **1** with  $\text{F}^-$  ions, which clearly showed the formation of H-bonded complex **1**• $\text{F}^-$  excluding any interactions with the B center. Titration of molecules **2** and **3** with complementary H-bonding **NAP** and **DAN** showed that heteromolecular H-bonded complexes **2**•**NAP**, **3**•**NAP** and **3**•**DAN** could be formed. In particular, complex **3**•**DAN** presents a quadruply H-bonded array with a  $K_a$  value of  $1820 \pm 130 \text{ M}^{-1}$  in  $\text{CDCl}_3$ . These findings open new applicative horizons for the BN-doping of polyaromatic hydrocarbons in supramolecular chemistry, for which the ability to form H-bonding interactions at the periphery can be exploited both in solution and at the solid state.<sup>41</sup> In addition, the ease of preparing these BN-doped PAHs makes these heterocycles interesting to organic, supramolecular and materials chemists who are incessantly looking for programmable synthetic strategies for digitizing molecules displaying multifunctional and self-organization properties exploitable in materials science and biology.<sup>42</sup>

## EXPERIMENTAL PART

Instrumentation, materials and general methods

**Thin layer chromatography (TLC):** performed on *Machevery-Nagel* Alugram SIL G/UV<sub>234</sub> 0.20 mm, visualized by UV light (254 or 366 nm). **Micro-wave irradiation (MW Irr.):** performed with a *Biotage* AB Initiator 2.5, in 2, 5 and 20 mL sealed tubes, producing controlled irradiation at 2.450 GHz. The reactions temperature was monitored with an external surface sensor. **Adsorption silica chromatography columns (SCC):** performed on *Merck Gerduran* silica gel 60 (40-63  $\mu$ m), used with a *Büchi* Sepacore X50 flash system. **Melting points (M.P.):** recorded on a *Büchi* Melting Point B-545 in open capillaries without correction. **Nuclear magnetic resonance analysis (<sup>1</sup>H, <sup>13</sup>C, <sup>11</sup>B-NMR):** spectra were recorded on a *Jeol* JNM EX-400, *Jeol* JNM ECZR-500, Bruker Fourier 300 MHz spectrometer equipped with a dual (<sup>13</sup>C, <sup>1</sup>H) probe, Bruker AVANCE III HD 400MHz NMR spectrometer equipped with a Broadband multinuclear (BBFO) SmartProbe™, a Bruker AVANCE III HD 500 MHz Spectrometer or a Bruker 600 MHz Advance 3 equipped with Broadband multinuclear (BBO) Prodigy CryoProbe. For <sup>1</sup>H and <sup>13</sup>C, chemical shifts are reported in ppm downfield from tetramethylsilane using the residual solvent signals as an internal reference (CDCl<sub>3</sub>  $\delta$ <sub>H</sub> = 7.26 ppm,  $\delta$ <sub>C</sub> = 77.16 ppm; CD<sub>2</sub>Cl<sub>2</sub>  $\delta$ <sub>H</sub> = 5.32 ppm,  $\delta$ <sub>C</sub> = 53.84 ppm. For <sup>11</sup>B, chemical shifts are reported in ppm downfield from BF<sub>3</sub>·OEt<sub>2</sub> as internal reference, and analyses were performed in quartz tubes. Coupling constants (J) are given in Hz. The resonance multiplicity is described as *s* singlet, *d* doublet, *t* triplet, *q* quartet, *dd* doublet of doublet, *m* multiplet and *br* broadened signal. All spectra were recorded at 25°C unless specified otherwise. **Ultraviolet-visible absorption spectroscopy (UV-Vis) and emission:** UV-Vis absorption spectra were recorded on Agilent Cary 5000 UV-Vis-NIR Spectrophotometer. All absorption measurements were performed at 25 °C unless specified otherwise. The estimated experimental errors are 2 nm on the band maximum, 5% on the molar absorption coefficient and 10% on the emission quantum yield in solution. Emission spectra were recorded on an Agilent Cary Eclipse fluorescence spectrofluorimeter. All fluorimetric measurements were performed at 25 °C unless specified otherwise. Quantum yield values in solution are calculated using anthracene in air equilibrated ethanol ( $\Phi$  = 0.27),<sup>43</sup> following the method of Demas and Crosby.<sup>44</sup> **Infrared absorption spectra (IR):** spectra were recorded on a) *Perkin-Elmer* Spectrum II FT-IR System UATR, mounted with a diamond crystal. Selected absorption bands are reported by wavenumber (cm<sup>-1</sup>). b) *Shimadzu* IR Affinity iS FTIR spectrometer in ATR mode with a diamond mono-crystal. **Matrix-assisted laser desorption-ionisation time-of-flight mass spectrometry analysis (MALDI-TOF):** Performed by a) the Centre de spectrométrie de masse at the Université de Mons in Belgium, using the following instrumentation: *Waters* QToF Premier mass spectrometer equipped with a nitrogen laser, operating at 337 nm with a maximum output of 500 mW delivered to the sample in 4 ns pulses at 20 Hz repeating rate. Time-of-flight analyses were performed in the reflectron mode at a resolution of about 10.000. The matrix solution (1  $\mu$ L) was applied to a stainless-steel target and air dried. Analyte samples were dissolved in a suitable solvent to obtain 1 mg/mL solutions. 1  $\mu$ L aliquots of these solutions were applied onto the target area already bearing the matrix crystals, and air dried. For the recording of the single-stage MS spectra, the quadrupole (rf-only mode) was set to pass ions from 100 to 1000 THz and all ions were transmitted into the pusher region of the time-of-flight analyser where they were analysed with 1 s integration time. **Electron spray ionization time of flight mass spectrometry analysis (ESI-TOF):** Performed at Cardiff University using a *Waters* LCT HR TOF mass spectrometer in the positive or negative ion mode for High-resolution ESI mass spectra.

#### Calculations:

DFT calculations were performed using the ab initio pseudopotential plane-wave method as implemented in the PWSCF code of the Quantum ESPRESSO distribution,<sup>45</sup> using ultrasoft pseudopotentials from the publicly available repository.<sup>46</sup> For the exchange-correlation term, a GGA-BLYP approximation has been used.<sup>47,48</sup> The valence electronic wave functions were expanded onto a plane wave basis set with a kinetic energy cutoff of 544 eV. The Brillouin zone integration for the gas-phase systems investigated has been limited to the  $\Gamma$ -point only. Ball and stick models are rendered using the XCrySDen software.<sup>49</sup>

#### Reagents and Solvents:

Reagents were purchased from *Sigma-Aldrich*, *Acros Organics*, *Fisher Scientific*, *Tokyo Chemical Industry (TCI Europe)*, *ABCR*, *Carbosynth*, and/or *Apollo Scientific* and used as received unless noted otherwise. NAP (1,8 naphthyridine) was acquired from

*fluorochem* or *TCI* and used as received. Solvents were purchased from *Sigma-Aldrich*, while deuterated solvents from *Eurisotop*. Anhydrous conditions were obtained by heating glassware in an oven at 120°C for 4 hours or by three cycles of heating with a heat gun under argon or nitrogen flow and cooling down under vacuum. The inert atmosphere was maintained using argon or nitrogen-filled balloons connected to a syringe and needle penetrating rubber stoppers used to close the flasks' necks. Solutions were degassed using freeze-pump-thaw technique: solutions were frozen using liquid nitrogen and kept under vacuum for 10' before thawing. ODCB (o-dichlorobenzene) was distilled from CaH<sub>2</sub> with reduced pressure and stored over 5 Å molecular sieves. All reactions were performed under anhydrous and inert gas conditions unless specified. Reactions were heated using silicon oil baths and the temperature monitored with an external probe unless otherwise specified.

## S2. Experimental procedures

### 4-(Phenylethynyl)aniline (4)

Diisopropylamine (80 mL) was degassed with 4 freeze-pump-thaw cycles in a flame-dried Schlenk. 4-iodoaniline (3.5 g, 16 mmol), [Pd(PPh<sub>3</sub>)<sub>2</sub>Cl<sub>2</sub>] (112 mg, 0.16 mmol), CuI (61 mg, 0.32 mmol) and phenylacetylene (2.11 mL, 19.2 mmol) were added, and the suspension stirred overnight at rt under argon. The black suspension was diluted with EtOAc (100 mL), washed with H<sub>2</sub>O (3 × 100 mL) and brine (100 mL). The organic phase was dried on Na<sub>2</sub>SO<sub>4</sub> and evaporated to a dark brown solid, purification by SCC (Cy/EtOAc 0 to 20%) afforded compound **4** as a white solid<sup>31</sup> (3.5 g, 99%). **M.P.**: 119–121°C. **<sup>1</sup>H-NMR** (400 MHz, CDCl<sub>3</sub>): δ 3.82 (*br s*, 2H), 6.64 (*d*, 2H, *J* = 8.8 Hz), 7.29–7.35 (*m*, 5H), 7.50 (*dd*, 2H, *J* = 8.0 Hz, *J*<sub>2</sub> = 1.4 Hz). **<sup>13</sup>C{<sup>1</sup>H}-NMR** (100 MHz, CDCl<sub>3</sub>): δ 87.4, 90.3, 112.4, 114.8, 123.9, 127.7, 128.4, 131.4, 133.0, 146.8. **IR**: 472, 498, 518, 535, 690, 756, 826, 846, 914, 966, 1068, 1137, 1179, 1290, 1317, 1371, 1440, 1486, 1513, 1591, 1615, 2210, 3036, 3377, 3475 cm<sup>-1</sup>. **HRMS** (EI-TOF) *m/z*: [M]<sup>+</sup> calcd. for C<sub>14</sub>H<sub>11</sub>N<sup>+</sup> 193.0886; found: 193.0888.

### 4-Phenethylaniline (5)

4-(phenylethynyl)aniline **4** (2.42 g, 12.5 mmol) was dissolved in MeOH (50 mL) under argon atmosphere, and Pd/C (10%, 267 mg, 0.25 mmol) added. Argon was replaced with H<sub>2</sub> and the suspension stirred at rt for 24 h. The reaction mixture was filtered on a celite pad and evaporated to a yellow residue, purification on a silica plug (Cy/EtOAc 30%) afforded molecule **5** as a white solid (2.44 g, quant.). **M.P.**: 51–53°C. **<sup>1</sup>H-NMR** (400 MHz, CDCl<sub>3</sub>): δ 2.65 (*m*, 4H), 3.48 (*br*, 2H), 6.63 (*d*, 2H, *J* = 8.4 Hz), 6.98 (*d*, 2H, *J* = 8.4 Hz), 7.17–7.30 (*m*, 5H). **<sup>13</sup>C{<sup>1</sup>H}-NMR** (100 MHz, CDCl<sub>3</sub>): δ 37.1, 38.3, 115.2, 125.8, 128.3, 128.5, 129.2, 131.8, 142.1, 144.4. **IR**: 523, 696, 747, 764, 810, 858, 1027, 1065, 1143, 1175, 1261, 1451, 1491, 1512, 1616, 2849, 2912, 3023, 3348 cm<sup>-1</sup>. **HRMS** (AP-TOF) *m/z*: [M+H]<sup>+</sup> calcd. for C<sub>14</sub>H<sub>16</sub>N<sup>+</sup>: 198.1283; found: 198.1285.

### 2-Bromo-4-phenethylaniline (6)

4-phenethylaniline **5** (1.7 g, 8.6 mmol) was stirred in CH<sub>3</sub>CN (60 mL) with NBS (1.5 g, 8.6 mmol) overnight. The solution was diluted with EtOAc (150 mL), washed with Na<sub>2</sub>S<sub>2</sub>O<sub>3</sub> sat. (100 mL), H<sub>2</sub>O (100 mL × 2), brine (100 mL), dried on MgSO<sub>4</sub> and evaporated. The residue was purified by SCC (Pet. Et/EtOAc 0 to 5%) to afford molecule **6** as a pale brown solid (2.0 g, 85%). **M.P.**: 47–49°C. **<sup>1</sup>H-NMR** (400 MHz, CD<sub>2</sub>Cl<sub>2</sub>): δ 2.79–2.88 (*m*, 4H), 4.00 (*bs*, 2H), 6.69 (*d*, 1H, *J* = 8.0 Hz), 6.93 (*dd*, 1H, *J* = 8.0 Hz, *J*<sub>2</sub> = 1.4 Hz), 7.18–7.31 (*m*, 6H). **<sup>13</sup>C{<sup>1</sup>H}-NMR** (100 MHz, CD<sub>2</sub>Cl<sub>2</sub>): δ 36.6, 38.0, 108.9, 115.7, 125.9, 128.3, 128.5, 128.6, 132.2, 133.1, 141.8, 142.3. **IR**: 481, 498, 560, 602, 675, 696, 739, 814, 889, 1033, 1079, 1155, 1202, 1265, 1305, 1411, 1452, 1496, 1600, 1616, 1711, 2856, 2922, 3026, 3336, 3420 cm<sup>-1</sup>. **HRMS** (EI-TOF) *m/z*: [M]<sup>+</sup> calcd. for C<sub>14</sub>H<sub>14</sub>BrN<sup>+</sup> 275.0304; found: 275.0307

### 1,3-Bis(4,4,5,5-tetramethyl-1,3,2-dioxaborolan-2-yl)benzene (12)



Anhydrous DMF (20 mL) was degassed with 5 freeze-pump-thaw cycles in a flame dried Schlenk. B<sub>2</sub>pin<sub>2</sub> (6.5 g, 25.4 mmol), [Pd(dppf)Cl<sub>2</sub>].CH<sub>2</sub>Cl<sub>2</sub> (350 mg, 0.43 mmol) and AcOK (3.3 g, 33.6 mmol) were added and 3 freeze-pump-thaw cycles performed. 1,3- dibromobenzene (2.0 g, 8.48 mmol) was added and the suspension heated at 90°C for 2 days under argon. The crude was then quenched with H<sub>2</sub>O (50 mL) and diluted with EtOAc (100 mL). The organic phase was washed with H<sub>2</sub>O (3 × 100 mL), brine (100 mL), dried on Na<sub>2</sub>SO<sub>4</sub> and evaporated to a dark solid, purified by a silica plug (Cy/EtOAc 50%) to obtain molecule **12** as a yellow pasty solid (2.8 g, quant.). **M.P.**: 111-113°C. **<sup>1</sup>H-NMR** (400 MHz, CDCl<sub>3</sub>): δ 1.34 (s, 24H), 7.37 (t, 1H, *J* = 7.8 Hz), 7.90 (dd, 2H, *J* = 7.4 Hz *J*<sub>2</sub> = 1.4 Hz), 8.28 (s, 1H). **<sup>13</sup>C{<sup>1</sup>H}-NMR** (100 MHz, CDCl<sub>3</sub>): 25.0, 83.9, 127.2, 137.8, 141.4 (signal for carbon atom attached to boron atom absent due to quadrupolar relaxation). **<sup>11</sup>B{<sup>1</sup>H}-NMR** (128 MHz, CDCl<sub>3</sub>): δ 29.5 (br). **IR**: 495, 519, 553, 578, 645, 653, 674, 685, 707, 807, 830, 845, 876, 951, 964, 983, 1009, 1079, 1110, 1138, 1214, 1270, 1305, 1328, 1370, 1456, 1474, 1602, 1669, 2934, 2978, 3436 cm<sup>-1</sup>. **HRMS** (ESI-TOF) *m/z*: [M+H]<sup>+</sup> calcd. for C<sub>18</sub>H<sub>29</sub>B<sub>2</sub>O<sub>4</sub><sup>+</sup> 331.2253; found: 331.2252. Characterization in accordance with data reported in the literature.<sup>40</sup>

#### 5,5''-Diphenethyl-[1,1':3',1''-terphenyl]-2,2''-diamine (**13**)

2-bromo-4-phenethylamine **6** (1.89 g, 6.87 mmol), diboronic ester **12** (754 mg, 2.28 mmol), Pd(OAc)<sub>2</sub> (26 mg, 0.11 mmol), SPhos (94 mg, 0.23 mmol) and KOAc (968 mg, 9.86 mmol) were dissolved in a 5:1 mixture of 1,4-dioxane (30 mL) and H<sub>2</sub>O (6 mL). The solution was degassed by 5 freeze-pump-thaw cycles and stirred at 80°C for 48 h under argon. The reaction mixture was allowed to cool down to rt, diluted with EtOAc (50 mL) and washed with H<sub>2</sub>O (50 mL × 3) and brine (100 mL). The organic layer was dried and the solvent evaporated under reduced pressure. The black residue was purified by SCC (Cy/EtOAc 0 to 15%) to yield compound **13** as a light yellow powder (770 mg, 71%) **M.P.**: 120-122°C. **<sup>1</sup>H-NMR** (400 MHz, CD<sub>2</sub>Cl<sub>2</sub>): δ 2.80-2.91 (*m*, 8H), 3.76 (*br s*, 4H), 6.70 (*d*, 2H, *J* = 7.6 Hz), 6.97-6.99 (*m*, 4H), 7.13-7.27 (*m*, 10H), 7.40-7.52 (*m*, 4H). **<sup>13</sup>C{<sup>1</sup>H}-NMR** (100 MHz, CD<sub>2</sub>Cl<sub>2</sub>): δ 37.6, 38.8, 116.2, 126.3, 127.6, 128.1, 128.8, 129.0, 129.1, 129.6, 130.2, 131.0, 132.4, 140.9, 142.2, 142.7. **IR**: 477, 499, 573, 617, 632, 695, 711, 741, 758, 817, 839, 895, 896, 908, 1029, 1089, 1154, 1251, 1269, 1299, 1307, 1386, 1451, 1469, 1504, 1601, 1617, 2854, 2920, 3025, 3354, 3440 cm<sup>-1</sup>. **HRMS** (EI-TOF) *m/z*: [M]<sup>+</sup> calcd. for C<sub>34</sub>H<sub>32</sub>N<sub>2</sub><sup>+</sup> 468.2560; found: 468.2567.

#### 5,12-Diphenethyl-8H,9H-8,9-diaza-8a-borabenzofg]tetracene (**1**)

A solution of BCl<sub>3</sub> (1.0 M in heptane, 250 μL, 0.25 mmol) was added to a solution of terphenyldiamine **6** (100 mg, 0.21 mmol) in anhydrous ODCB (6 mL). The reaction mixture was stirred for 15 min at rt under N<sub>2</sub> before adding AlCl<sub>3</sub> (3 mg, 0.023 mmol) and then heated at 150°C under microwave irradiation for 16 h. The solution was allowed to cool down to rt and the solvent removed from the deep brown solution under reduced pressure. The residue was purified by SCC (Cy/EtOAc 0 to 10%) to yield molecule **1** as a white powder (50 mg, 49%). **M.P.**: 194-196°C. **<sup>1</sup>H-NMR** (400 MHz, DMSO-*d*<sub>6</sub>, 50°C): δ 2.96 (*m*, 8 H), 7.14-7.29 (*m*, 14H) 7.76 (*t*, 1H, *J* = 7.9 Hz), 8.00 (*s*, 2H), 8.09 (*s*, 2H), 8.17 (*d*, 2H, *J* = 7.9 Hz). **<sup>13</sup>C{<sup>1</sup>H}-NMR** (100 MHz, DMSO-*d*<sub>6</sub>): δ 37.4, 38.2, 118.8, 119.1, 121.5, 124.3, 126.3, 128.8, 129.0, 129.2, 131.2, 132.5, 139.3, 140.1, 142.5. (signal for carbon atom attached to boron atom absent due to quadrupolar relaxation). **<sup>11</sup>B{<sup>1</sup>H}-NMR** (128 MHz, DMSO-*d*<sub>6</sub>): δ 26.5. **IR**: 531, 580, 628, 649, 670, 699, 750, 750, 798, 849, 875, 916, 1029, 1075, 1288, 1319, 1340, 1420, 1444, 1453, 1468, 1497, 1560, 1603, 2918, 3292 cm<sup>-1</sup>. **HRMS** (EI-TOF) *m/z*: [M]<sup>+</sup> calcd. for C<sub>34</sub>H<sub>29</sub>BN<sub>2</sub><sup>+</sup> 476.2418; found: 476.2413.

#### 5-Mesitylpyridin-2-amine (**10**)

2-amino-5-bromopyridine (1.0 g, 5.8 mmol), 2,4,6-trimethylphenylboronic acid (1.1 g, 6.7 mmol), Pd(OAc)<sub>2</sub> (70 mg, 0.31 mmol), XPhos (429 mg, 0.90 mmol) and K<sub>3</sub>PO<sub>4</sub> (3.7 g, 17.4 mmol) were dissolved in a 5:1 mixture of 1,4-dioxane (10 mL) and H<sub>2</sub>O (2 mL). The

solution was degassed by 3 freeze-pump-thaw cycles and stirred at 90°C for 48 h under nitrogen. The reaction mixture was allowed to cool down to rt, diluted with EtOAc (50 mL), washed with H<sub>2</sub>O (50 mL × 3) and brine (100 mL). The organic layer was dried over MgSO<sub>4</sub> and the solvent evaporated under reduced pressure. The black residue was purified by SCC (Pet. Et./EtOAc 0 to 30%) to yield compound **10** as an orange powder (1.17 g, 95%). **M.P.**: 92–94°C; **<sup>1</sup>H-NMR** (300 MHz, CDCl<sub>3</sub>): δ 2.04 (s, 6H), 2.32 (s, 3H), 4.50 (bs, 2H), 6.59 (d, 1H, *J* = 8.7 Hz), 6.94 (s, 2H), 7.25 (dd, 1H, *J*<sub>1</sub> = 8.7 Hz, *J*<sub>2</sub> = 1.2 Hz), 7.87 (d, 1H, *J* = 1.2 Hz). **<sup>13</sup>C{<sup>1</sup>H}-NMR** (75 MHz, CDCl<sub>3</sub>): δ 21.0, 21.1, 108.5, 126.8, 128.3, 135.5, 137.0, 137.1, 139.2, 148.2, 157.1. **IR**: 407, 421, 571, 754, 835, 847, 912, 1011, 1057, 1146, 1234, 1315, 1387, 1439, 1468, 1624, 2913, 3140, 3285, 3464. **HRMS** (EI-TOF) *m/z*: [M]<sup>+</sup> calcd. for C<sub>14</sub>H<sub>16</sub>N<sub>2</sub><sup>+</sup> 212.1308; found 212.1313.

### 3-Bromo-5-mesitylpyridin-2-amine (**11**)

5-mesitylpyridin-2-amine **10** (260 mg, 1.22 mmol) was stirred in CH<sub>3</sub>CN (20 mL) with NBS (220 mg, 1.23 mmol) overnight. The solution was diluted in CH<sub>2</sub>Cl<sub>2</sub> (30 mL), washed with sat. Na<sub>2</sub>S<sub>2</sub>O<sub>3</sub> (50 mL), H<sub>2</sub>O (50 mL × 3), brine (50 mL), dried over MgSO<sub>4</sub> and evaporated. The resulting residue was purified by SCC (Pet. Et./EtOAc 0 to 30%) to afford molecule **11** as a pale yellow solid (310 mg, 87%). **M.P.**: 138–140°C; **<sup>1</sup>H-NMR** (300 MHz, CDCl<sub>3</sub>): δ 2.05 (s, 6H), 2.32 (s, 3H), 5.02 (*br s*, 2H), 6.94 (s, 2H), 7.50 (d, 1H, *J* = 1.2 Hz), 7.83 (d, 1H, *J* = 1.2 Hz). **<sup>13</sup>C{<sup>1</sup>H}-NMR** (75 MHz, CDCl<sub>3</sub>): δ 21.0, 21.2, 104.4, 128.2, 128.6, 134.2, 137.1, 137.6, 141.5, 147.5, 154.2. **IR**: 413, 422, 434, 498, 534, 579, 625, 710, 745, 754, 853, 881, 912, 939, 951, 1011, 1057, 1234, 1267, 1288, 1389, 1441, 1468, 1489, 1533, 1593, 1632, 2853, 2916, 3136, 3285, 3470. **HRMS** (EI-TOF) *m/z*: [M+H]<sup>+</sup> calcd. for C<sub>14</sub>H<sub>16</sub>BrN<sub>2</sub><sup>+</sup> 291.0491; found: 291.0499.

### 3,3'-(1,3-Phenylene)bis(5-mesitylpyridin-2-amine) (**15**)

3-bromo-5-mesitylpyridin-2-amine **11** (200 mg, 0.69 mmol), diboronic ester **12** (113 mg, 0.34 mmol), Pd(OAc)<sub>2</sub> (4 mg, 0.02 mmol), XPhos (32 mg, 0.07 mmol) and K<sub>3</sub>PO<sub>4</sub> (437 mg, 2.06 mmol) were dissolved in a 5:1 mixture of 1,4-dioxane (5 mL) and H<sub>2</sub>O (1 mL). The solution was degassed by 5 freeze-pump-thaw cycles and stirred at 90°C for 20 h under argon. The reaction mixture was allowed to cool down to rt, diluted with CH<sub>2</sub>Cl<sub>2</sub> (50 mL) and washed with H<sub>2</sub>O (40 mL × 3) and brine (50 mL). The organic layer was dried over MgSO<sub>4</sub> and the solvent evaporated under reduced pressure. The black residue was purified by SCC (Pet. Et./EtOAc 30 to 90%)<sup>\*</sup> to yield compound **15** as a light brown solid (230 mg, 67%). **M.P.**: 248–250 °C; **<sup>1</sup>H-NMR** (300 MHz, CDCl<sub>3</sub>): δ 2.09 (s, 12H), 2.32 (s, 6H), 4.65 (*br s*, 4H), 6.95 (s, 4H), 7.25 (d, 2H, *J* = 2.1 Hz), 7.53–7.61 (*m*, 4H), 7.90 (d, 2H, *J* = 2.1 Hz). **<sup>13</sup>C{<sup>1</sup>H}-NMR** (75 MHz, CDCl<sub>3</sub>): δ 21.2, 121.2, 127.6, 128.2, 128.4, 129.2, 130.0, 135.1, 137.0, 137.2, 139.2, 139.4, 147.6, 154.4. (one signal not visible due to overlapping). **IR**: 411, 426, 494, 538, 573, 635, 714, 793, 849, 912, 1005, 1229, 1391, 1454, 1491, 1558, 1622, 2918, 3140, 3283, 3493. **HRMS** (EI-TOF) *m/z*: [M]<sup>+</sup> calcd. for C<sub>34</sub>H<sub>34</sub>N<sub>4</sub><sup>+</sup> 498.2778; found 498.2783.<sup>\*</sup> 5% Et<sub>3</sub>N was added to the final eluent to recover the product from the column.

### 5,12-Dimesityl-8H,9H-7,8,9,10-tetraaza-8a-borabenzofg]tetracene (**3**)

A solution of BCl<sub>3</sub> (1.0 M in heptane, 210 μL, 0.21 mmol) was added to a solution of terphenyldiamine **15** (100 mg, 0.20 mmol) in anhydrous ODCB (6 mL). The reaction mixture was stirred for 15 min at rt under N<sub>2</sub> before adding AlCl<sub>3</sub> (3 mg, 0.023 mmol) and heating at 150°C under microwave irradiation for 16 h. The solution was allowed to cool down to rt and the solvent removed from the deep brown solution under reduced pressure. The residue was purified by SCC (Pet. Et./EtOAc 30 to 60%)<sup>\*</sup> to yield molecule **3** as a white powder (17 mg, 17%). **M.P.**: 196–198 °C **<sup>1</sup>H-NMR** (300 MHz, CDCl<sub>3</sub>): δ 2.11 (s, 12H, *CH<sub>c</sub>*), 2.37 (s, 6H, *CH<sub>e</sub>*), 7.02 (s, 4H, *CH<sub>d</sub>*), 7.44 (*bs*, 2H, *NH<sub>f</sub>*), 7.79 (*t*, 1H, *J* = 7.9 Hz, *CH<sub>h</sub>*), 8.11 (d, 2H, *J* = 7.9 Hz, *CH<sub>g</sub>*), 8.15 (d, 2H, *J* = 2.0 Hz, *CH<sub>a</sub>*), 8.31 (d, 2H, *J* = 2.0 Hz, *CH<sub>b</sub>*). **<sup>13</sup>C{<sup>1</sup>H}-NMR** (126 MHz, CDCl<sub>3</sub>): δ 21.2, 117.4, 120.3, 128.5, 129.5, 131.5, 133.5, 135.4, 137.1, 137.6, 138.4, 148.3, 150.9. (signal for carbon atom attached to boron atom absent due to quadrupolar relaxation, one signal for *CH<sub>c</sub>* *CH<sub>e</sub>* not visible due to overlapping).

**<sup>1</sup>B{<sup>1</sup>H}-NMR** (160 MHz, CDCl<sub>3</sub>): δ: 27.7. **IR:** 581, 822, 851, 910, 1233, 1281, 1387, 1447, 1576, 1611, 2853, 2920, 2955, 3059, 3221, 3364. **HRMS** (ESI-TOF) m/z: [M+H]<sup>+</sup> calcd. for C<sub>34</sub>H<sub>32</sub>BN<sub>4</sub><sup>+</sup> 507.2709; found 507.2710 \*Addition of 5 % MeOH to the last eluent was required to remove all product from the column.

#### 2,4,6-Trimethyl-4'-nitro-1,1'-biphenyl (7)

4-bromonitrobenzene (500 mg, 2.49 mmol), 2,4,6-trimethylphenylboronic acid (447 mg, 2.72 mmol), [Pd(PPh<sub>3</sub>)<sub>4</sub>](287 mg, 0.25 mmol), and K<sub>2</sub>CO<sub>3</sub> (1.03 g, 7.46 mmol) were dissolved in a 5:1 mixture of 1,4-dioxane (10 mL) and H<sub>2</sub>O (2 mL). The solution was degassed by 3 freeze-pump-thaw cycles and stirred at 90°C for 48 h under nitrogen. The reaction mixture was allowed to cool down to rt, diluted with CH<sub>2</sub>Cl<sub>2</sub> (50 mL), washed with H<sub>2</sub>O (100 mL × 3) and brine (100 mL). The organic layer was dried over MgSO<sub>4</sub> and the solvent evaporated under reduced pressure. The residue was purified by SCC (Pet. Et/CH<sub>2</sub>Cl<sub>2</sub> 0 to 20%) to yield compound **7** as a yellow powder (350 mg, 58%). **<sup>1</sup>H-NMR** (300 MHz, CDCl<sub>3</sub>): δ 2.01 (s, 6H), 2.36 (s, 3H), 6.99 (s, 2H), 7.35 (d, 2H, *J* = 8.8 Hz), 8.31 (d, 2H, *J* = 8.8 Hz). **<sup>13</sup>C{<sup>1</sup>H}-NMR** (75 MHz, CDCl<sub>3</sub>): δ 20.7, 21.1, 123.9, 128.5, 130.6, 135.4, 136.9, 137.8, 147.0, 148.7. **IR:** 409, 440, 471, 511, 525, 571, 579, 594, 700, 731, 739, 760, 827, 851, 959, 1005, 1028, 1067, 1098, 1105, 1177, 1283, 1312, 1344, 1385, 1396, 1472, 1514, 1599, 1927, 2849, 2947, 3013, 3104. **HRMS** (EI-TOF) m/z: [M]<sup>+</sup> calcd for C<sub>15</sub>H<sub>15</sub>NO<sub>2</sub><sup>+</sup> 241.1097; found 241.1108.

#### 2,4,6-Trimethyl-4'-amino-1,1'-biphenyl (8)

Compound **7** (350 mg, 1.45 mmol) was suspended in a EtOH (15 mL) AcOH (3 mL) solution and stirred for 2 h at rt in the presence of Zn (948 mg, 14.5 mmol). The suspension was filtered through celite to remove the excess of Zn while washing with EtOAc (100 mL). The organic layers were washed with Sat. K<sub>2</sub>CO<sub>3</sub> (100 mL × 2), brine (100 mL) dried over MgSO<sub>4</sub>, filtered and evaporated under reduced pressure. The yellowish residue was purified by SCC (Pet. Et/EtOAc 20 to 60%) to yield compound **8** as a pale yellow powder (270 mg, 88%) **<sup>1</sup>H-NMR** (300 MHz, CDCl<sub>3</sub>): δ 2.03 (s, 6H), 2.32 (s, 3H), 3.92 (*br s*, 2H), 6.77 (d, 2H, *J* = 8.5 Hz), 6.92-6.98 (*m*, 4H). **<sup>13</sup>C{<sup>1</sup>H}-NMR** (75 MHz, CDCl<sub>3</sub>): δ 21.0, 21.1, 115.5, 128.1, 130.3, 131.7, 136.3, 136.7, 139.1, 144.4. **IR:** 415, 440, 511, 540, 579, 702, 739, 760, 851, 1005, 1098, 1105, 1177, 1283, 1312, 1344, 1385, 1474, 1514, 1599, 2851, 2918, 2949, 3011, 3352, 3431. **HRMS** (EI-TOF) m/z: [M+H]<sup>+</sup> calcd. for C<sub>15</sub>H<sub>18</sub>N<sup>+</sup> 212.1432; found 212.1435.

#### 3-Bromo-2',4',6'-trimethyl-[1,1'-biphenyl]-4-amine (9)

4-mesitylaniline **8** (270 mg, 1.28 mmol) was dissolved in CHCl<sub>3</sub> (10 mL) and NBS (228 mg, 1.28 mmol) added at 0°C. The reaction was allowed to reach r.t. and stirred overnight. The solution was diluted in EtOAc (100 mL), washed with Na<sub>2</sub>S<sub>2</sub>O<sub>3</sub> sat. (50 mL), H<sub>2</sub>O (100 mL × 3), brine (100 mL), dried over MgSO<sub>4</sub> and evaporated. The orange residue was purified by SCC (Pet. Et/EtOAc 0 to 5%) to afford molecule **9** as a viscous transparent oil (277 mg, 75%). **<sup>1</sup>H-NMR** (300 MHz, CDCl<sub>3</sub>): δ 2.02 (s, 6H), 2.31 (s, 3H), 4.57 (*br s*, 2H), 6.88-6.89 (*m*, 2H), 6.92 (s, 2H), 7.21 (d, *J* = 1.8 Hz, 1H). **<sup>13</sup>C{<sup>1</sup>H}-NMR** (75 MHz, CDCl<sub>3</sub>): δ 20.9, 21.1, 109.4, 115.8, 128.1, 129.5, 132.5, 133.1, 136.5, 136.7, 137.7, 142.5. **IR:** 407, 434, 527, 577, 615, 658, 696, 731, 818, 851, 883, 908, 1015, 1040, 1153, 1240, 1267, 1288, 1302, 1375, 1395, 1474, 1508, 1616, 2855, 2916, 3011, 3375, 3472. **HRMS** (EI-TOF) m/z: [M+H]<sup>+</sup> calcd. for C<sub>15</sub>H<sub>17</sub>BrN<sup>+</sup>, 290.0539; found 290.0544.

#### 2,2''',4,4''',6,6'''-Hexamethyl-[1,1':3,1'':3'',1''':3''',1''''-quinquephenyl]-4',6'''-diamine (14)

3-bromo-2',4',6'-trimethyl-[1,1'-biphenyl]-4-amine **9** (500mg, 1.72 mmol), diboronic ester **12** (260 mg, 0.78 mmol), Pd(OAc)<sub>2</sub> (13 mg, 0.06 mmol), XPhos (47 mg, 0.10 mmol) and K<sub>3</sub>PO<sub>4</sub> (470 mg, 2.21 mmol) were dissolved in a 5:1 mixture of 1,4-dioxane (15 mL) and

H<sub>2</sub>O (3 mL). The solution was degassed by 5 freeze-pump-thaw cycles and stirred at 80 °C for 48 h under argon. The reaction mixture was allowed to cool down to rt, diluted with EtOAc (50 mL), washed with H<sub>2</sub>O (50 mL × 3) and brine (100 mL). The organic layer was dried over MgSO<sub>4</sub> and the solvent evaporated under reduced pressure. The black residue was purified by SCC (Pet. Et./EtOAc 30 to 90%) to yield compound **14** as a white-yellow powder (500 mg, 58%). **M.P.**: 112–114 °C; **<sup>1</sup>H-NMR** (300 MHz, CDCl<sub>3</sub>):

δ 2.09 (s, 12H), 2.32 (s, 6H), 3.86 (*br s*, 4H), 6.83 (*d*, 2H, *J* = 7.4 Hz), 6.92–6.97 (*m*, 8H), 7.48–7.53 (*m*, 3H), 7.61 (*s*, 1H). **<sup>13</sup>C{<sup>1</sup>H}-NMR** (75 MHz, CDCl<sub>3</sub>): δ 21.1, 21.1, 116.0, 127.5, 127.9, 128.2, 129.3, 129.7, 129.9, 131.4, 131.6, 136.3, 136.7, 139.0, 140.4, 142.0. **IR**: 573, 633, 729,

822, 907, 1013, 1030, 1152, 1287, 1375, 1472, 1508, 1616, 2857, 2916, 2947, 3015, 3368, 3460. **HRMS** (EI-TOF) *m/z*: [M+H]<sup>+</sup> calcd. for C<sub>36</sub>H<sub>36</sub>N<sub>2</sub><sup>+</sup> 497.2951; found 497.2950.

#### 5,12-Dimesityl-8H,9H-8,9-diaza-8a-borabenzofg]tetracene (**2**)

A solution of BCl<sub>3</sub> (1.0 M in heptane, 210 μL, 0.21 mmol) was added to a solution of terphenyldiamine **14** (100 mg, 0.20 mmol) in anhydrous ODCB (6 mL). The reaction mixture was stirred for 15 min at rt under N<sub>2</sub> before adding AlCl<sub>3</sub> (3 mg, 0.023 mmol) and heating at 150 °C under microwave irradiation for 16 h. The solution was allowed to cool down to rt and the solvent removed from the deep brown solution under reduced pressure. The residue was purified by SCC (Pet. Et./EtOAc 30 to 60%) to yield molecule **2** as a white powder (50 mg, 50%). **M.P.**: 156–158 °C; **<sup>1</sup>H-NMR** (300 MHz, CDCl<sub>3</sub>): δ 2.12 (*s*, 12H, CH<sub>c</sub>), 2.38 (*s*, 6H, CH<sub>e</sub>), 6.33 (*bs*, 2H, NH<sub>f</sub>), 7.01 (*s*, 4H, CH<sub>d</sub>), 7.08–7.13 (*m*, 4H, CH<sub>ai</sub>), 7.74 (*t*, 1H, *J* = 8.0 Hz, CH<sub>h</sub>), 8.04 (*s*, 2H, CH<sub>b</sub>), 8.10 (*d*, 2H, *J* = 7.9 Hz, CH<sub>g</sub>). **<sup>13</sup>C{<sup>1</sup>H}-NMR** (126 MHz, CDCl<sub>3</sub>): δ 21.15, 21.21, 118.4, 119.2, 122.5, 125.3, 128.3, 129.6, 131.2, 132.7, 136.7, 136.8, 139.2, 139.2, 139.3. (signal for carbon atom attached to boron atom absent due to quadrupolar relaxation) **<sup>11</sup>B{<sup>1</sup>H}-NMR** (160 MHz, CDCl<sub>3</sub>): δ 27.0. **IR**: 405, 490, 581, 619, 638, 673, 750, 822, 851, 889, 1028, 1076, 1138, 1188, 1221, 1256, 1283, 1298, 1321, 1375, 1406, 1447, 1460, 1572, 2853, 2916, 2953, 3007, 3385. **HRMS** (AP-TOF) *m/z*: [M+H]<sup>+</sup> calcd. for C<sub>36</sub>H<sub>34</sub><sup>10</sup>BN<sub>2</sub><sup>+</sup> 504.2851; found 504.2833.

## ASSOCIATED CONTENT

### Supporting Information

Synthetic protocols and spectroscopic data for all molecules, computational studies, electrochemical characterization and titration experiments. The Supporting Information is available free of charge on the ACS Publications website at DOI: TO BE ADDED.

## AUTHOR INFORMATION

**Corresponding Author\*** E-mail: bonifazid@cardiff.ac.uk

## ACKNOWLEDGMENTS

The authors gratefully acknowledge the EU through the ERC Starting Grant “COLORLANDS” and the FRS-FNRS. JT thanks the FRIA (FNRS) for his doctoral fellowship. DB is grateful to the RW through the FLYCOAT project and to Cardiff University for generous funding. DB and PT thank the EU for the MC-RISE INFUSION research project. We thank T. Battisti at Cardiff University for the ESP calculations.

## REFERENCES

- (1) Narita, A.; Wang, X. Y.; Feng, X.; Müllen, K. New advances in nanographene chemistry. *Chem. Soc. Rev.* **2015**, *44* (18), 6616– 6643.
- (2) Helten, H. B=N Units as Part of Extended π-Conjugated Oligomers and Polymers. *Chem. Eur. J.* **2016**, *22* (37), 12972–12982.
- (3) Lorenzo-García, M. M.; Bonifazi, D. Renaissance of an Old Topic: From Borazines to BN-doped Nanographenes. *Chim. Int. J. Chem.* **2017**, *71* (9), 550–557.



- (4) Giustra, Z. X.; Liu, S. Y. The State of the Art in Azaborine Chemistry: New Synthetic Methods and Applications. *J. Am. Chem. Soc.* **2018**, *140* (4), 1184–1194.
- (5) Wang, X. Y.; Wang, J. Y.; Pei, J. BN heterosuperbenzenes: Synthesis and properties. *Chem. Eur. J.* **2015**, *21* (9), 3528–3539.
- (6) Liu, Z.; Marder, T. B. B-N versus C-C: How similar are they? *Angew. Chem. Int. Ed.* **2008**, *47* (2), 242–244.
- (7) Helten, H. Doping the Backbone of  $\pi$ -Conjugated Polymers with Tricoordinate Boron: Synthetic Strategies and Emerging Applications. *Chem. - An Asian J.* **2019**, *14* (7), 919–935.
- (8) Kervyn, S.; Fenwick, O.; Di Stasio, F.; Shin, Y. S.; Wouters, J.; Accorsi, G.; Osella, S.; Beljonne, D.; Cacialli, F.; Bonifazi, D. Polymorphism, fluorescence, and optoelectronic properties of a borazine derivative. *Chem. Eur. J.* **2013**, *19* (24), 7771–7779.
- (9) Bonifazi, D.; Fasano, F.; Lorenzo-Garcia, M. M.; Marinelli, D.; Oubaha, H.; Tasseroul, J. Boron–nitrogen doped carbon scaffolding: organic chemistry, self-assembly and materials applications of borazine and its derivatives. *Chem. Commun.* **2015**, *51* (83), 15222–15236.
- (10) Dewar, M. J. S.; Marr, P. A. A Derivative of Borazarene. *J. Am. Chem. Soc.* **1962**, *84* (19), 3782–3782.
- (11) Campbell, P. G.; Marwitz, A. J. V; Liu, S. Recent Advances in Azaborine Chemistry. *Angew. Chem. Int. Ed.* **2012**, *51* (25), 6074–6092.
- (12) Bosdet, M. J. D.; Piers, W. E.; Sorensen, T. S.; Parvez, M. 10a-Aza-10b-borapyrenes: Heterocyclic Analogues of Pyrene with Internalized BN Moieties. *Angew. Chem. Int. Ed.* **2007**, *46* (26), 4940–4943.
- (13) Chissick, S. S.; Dewar, M. J. S.; Maitlis, P. M. New heteraromatic compounds containing two boron atoms. *Tetrahedron Lett.* **1960**, *1* (44), 8–10.
- (14) Bosdet, M. J. D.; Jaska, C. A.; Piers, W. E.; Sorensen, T. S.; Parvez, M. Blue Fluorescent 4a-Aza-4b-boraphenanthrenes. *Org. Lett.* **2007**, *9* (7), 1395–1398.
- (15) Dewar, M. J. S.; Dietz, R. 546. New heteroaromatic compounds. Part III. 2,1-Borazaro-naphthalene (1,2-dihydro-1-aza-2-boranaphthalene). *J. Chem. Soc.* **1959**, 2728–2730.
- (16) Wisniewski, S. R.; Guenther, C. L.; Argintaru, O. A.; Molander, G. A. A Convergent, Modular Approach to Functionalized 2,1-Borazaronaphthalenes from 2-Aminostyrenes and Potassium Organotrifluoroborates. *J. Org. Chem.* **2014**, *79* (1), 365–378.
- (17) Ishibashi, J. S. A.; Marshall, J. L.; Mazie, A.; Lovinger, G. J.; Li, B.; Zakharov, L. N.; Dargelos, A.; Graciaa, A.; Chrostowska, A.; Liu, S. Two BN Isosteres of Anthracene: Synthesis and Characterization. *J. Am. Chem. Soc.* **2014**, *136*, 15414–15421.
- (18) van de Wouw, H. L.; Lee, J. Y.; Siegler, M. A.; Klausen, R. S. Innocent BN bond substitution in anthracene derivatives. *Org. Biomol. Chem.* **2016**, *14* (12), 3256–3263.
- (19) Fingerle, M.; Stocker, S.; Bettinger, H. F. New Synthesis of a Dibenzoperylene Motif Featuring a Doubly Boron–Nitrogen-Doped Bay Region. *Synthesis*. **2019**, *51*, 4147–4152.
- (20) Hatakeyama, T.; Hashimoto, S.; Seki, S.; Nakamura, M. Synthesis of BN-Fused Polycyclic Aromatics via Tandem Intramolecular Electrophilic Arene Borylation. *J. Am. Chem. Soc.* **2011**, *133* (46), 18614–18617.
- (21) Stępień, M.; Gońka, E.; Żyła, M.; Sprutta, N. Heterocyclic Nanographenes and Other Polycyclic Heteroaromatic Compounds: Synthetic Routes, Properties, and Applications. *Chem. Rev.* **2017**, *117* (4), 3479–3716.
- (22) For OLED applications see: a) Nakatsuka, S.; Hatakeyama, T.; Ikuta, T.; Kinoshita, K.; Nomura, S.; Ono, Y.; Ni, J.; Nakajima,

- K.; Shiren, K. Ultrapure Blue Thermally Activated Delayed Fluorescence Molecules: Efficient HOMO-LUMO Separation by the Multiple Resonance Effect. *Adv. Mater.* **2016**, *28* (14), 2777–2781; b) Fresta, E.; Dosso, J.; Cabanillas-González, J.; Bonifazi, D.; Costa, R. D. Origin of the Exclusive Ternary Electroluminescent Behavior of BN-Doped Nanographenes in Efficient Single-Component White Light-Emitting Electrochemical Cells. *Adv. Funct. Mater.* **2020**, DOI: 10.1002/adfm.201906830.
- (23) Georgiou, I.; Kervyn, S.; Rossignon, A.; De Leo, F.; Wouters, J.; Bruylants, G.; Bonifazi, D. Versatile Self-Adapting Boronic Acids for H-Bond Recognition: From Discrete to Polymeric Supramolecules. *J. Am. Chem. Soc.* **2017**, *139* (7), 2710–2727.
  - (24) Lee, H.; Fischer, M.; Shoichet, B. K.; Liu, S. Y. Hydrogen Bonding of 1,2-Azaborines in the Binding Cavity of T4 Lysozyme Mutants: Structures and Thermodynamics. *J. Am. Chem. Soc.* **2016**, *138* (37), 12021–12024.
  - (25) Liu, Y.; Liu, S.-Y. Exploring the strength of a hydrogen bond as a function of steric environment using 1,2-azaborine ligands and engineered T4 lysozyme receptors. *Org. Biomol. Chem.* **2019**, *17* (29), 7002–7006.
  - (26) Dosso, J.; Tasseroul, J.; Fasano, F.; Marinelli, D.; Biot, N.; Fermi, A.; Bonifazi, D. Synthesis and Optoelectronic Properties of Hexa-peri-hexabenzoborazinocoronene. *Angew. Chem. Int. Ed.* **2017**, *56* (16), 4483–4487.
  - (27) Numano, M.; Nagami, N.; Nakatsuka, S.; Katayama, T.; Nakajima, K.; Tatsumi, S.; Yasuda, N.; Hatakeyama, T. Synthesis of Boronate-Based Benzo[fg]tetracene and Benzo[hi]hexacene via Demethylative Direct Borylation. *Chem. - A Eur. J.* **2016**, *22*, 11574–11577.
  - (28) Wang, X.; Zhang, F.; Schellhammer, K. S.; Machata, P.; Ortmann, F.; Cuniberti, G.; Fu, Y.; Hunger, J.; Tang, R.; Popov, A. A.; et al. Synthesis of NBN-Type Zigzag-Edged Polycyclic Aromatic Hydrocarbons: 1,9-Diaza-9a-boraphenalene as a Structural Motif. *J. Am. Chem. Soc.* **2016**, *138* (36), 11606–11615.
  - (29) Ishibashi, J. S. A.; Marshall, J. L.; Mazière, A.; Lovinger, G. J.; Li, B.; Zakharov, L. N.; Dargelos, A.; Graciaa, A.; Chrostowska, A.; Liu, S. Y. Two BN isosteres of anthracene: Synthesis and characterization. *J. Am. Chem. Soc.* **2014**, *136* (43), 15414–15421.
  - (30) White, N. G. Recent advances in self-assembled amidinium and guanidinium frameworks. *Dalt. Trans.* **2019**, *48* (21), 7062–7068.
  - (31) Adjabeng, G.; Brenstrum, T.; Frampton, C. S.; Robertson, A. J.; Hillhouse, J.; McNulty, J.; Capretta, A. Palladium complexes of 1,3,5,7-tetramethyl-2,4,8-trioxa-6-phenyl-6-phosphaadamantane: Synthesis, crystal structure and use in the Suzuki and Sonogashira reactions and the  $\alpha$ -arylation of ketones. *J. Org. Chem.* **2004**, *69* (15), 5082–5086.
  - (32) Biswas, S.; Müller, M.; Tönshoff, C.; Eichele, K.; Maichle-Mössmer, C.; Ruff, A.; Speiser, B.; Bettinger, H. F. The overcrowded borazine derivative of hexabenzotriphenylene obtained through dehydrohalogenation. *Eur. J. Org. Chem.* **2012**, *24*, 4634–4639.
  - (33) Müller, M.; Behnle, S.; Maichle-Mössmer, C.; Bettinger, H. F. Boron–nitrogen substituted perylene obtained through photocyclisation. *Chem. Commun.* **2014**, *50* (58), 7821.
  - (34) Boiocchi, M.; Del Boca, L.; Gómez, D. E.; Fabbrizzi, L.; Licchelli, M.; Monzani, E. Nature of Urea–Fluoride Interaction: Incipient and Definitive Proton Transfer. *J. Am. Chem. Soc.* **2004**, *126* (50), 16507–16514.
  - (35) Esteban-Gómez, D.; Fabbrizzi, L.; Licchelli, M. Why, on Interaction of Urea-Based Receptors with Fluoride, Beautiful Colors Develop. *J. Org. Chem.* **2005**, *70* (14), 5717–5720.
  - (36) Goursaud, M.; De Bernardin, P.; Dalla Cort, A.; Bartik, K.; Bruylants, G. Monitoring fluoride binding in DMSO: Why is a singular binding behavior observed? *Eur. J. Org. Chem.* **2012**, *19*, 3570–3574.

- (37) Liang, F.; Lindsay, S.; Zhang, P. 1,8-Naphthyridine-2,7-diamine: A potential universal reader of Watson-Crick base pairs for DNA sequencing by electron tunneling. *Org. Biomol. Chem.* **2012**, *10* (43), 8654–8659.
- (38) Hunter, C. A. Quantifying intermolecular interactions: Guidelines for the molecular recognition toolbox. *Angew. Chem. Int. Ed.* **2004**, *43* (40), 5310–5324.
- (39) Kuzmič, P. Program DYNAFIT for the analysis of enzyme kinetic data: Application to HIV proteinase. *Anal. Biochem.* **1996**, *237* (2), 260–273.
- (40) Fu, S. H.; Higuchi, M.; Kurth, D. G. Diverse synthesis of novel bisterpyridines via Suzuki-type cross-coupling. *Org. Lett.* **2007**, *9* (4), 559–562.
- (41) Blight, B. A.; Hunter, C. A.; Leigh, D. A.; McNab, H.; Thomson, P. I. T. An AAAA-DDDD quadruple hydrogen-bond array. *Nature Chem.* **2011**, *3*, 244–248.
- (42) (a) Wilson, A. J. Hydrogen Bonding Receptors for Molecular Guests , in ‘Supramolecular Chemistry: From Molecules to Nanomaterials’ Vol 3, Ed. Enrique García-España , Series Eds. P.A . Gale, J. W. Steed, Wiley, **2012**, 1325-1344; (b) Wilson, A. J. Non-Covalent Polymer Assembly Using Arrays of Hydrogen-Bonds. *Soft Mat.*, **2007**, *3*, 409-425.
- (43) Würth, C.; Grabolle, M.; Pauli, J.; Spieles, M.; Resch-genger, U. Relative and absolute determination of fluorescence quantum yields of transparent samples. *Nat. protoc.* **2013**, *8* (8), 1535–1550.
- (44) Crosby, G. A.; Demas, J. N. Measurement of photoluminescence quantum yields. Review. *J. Phys. Chem.* **1971**, *75* (8), 991–1024.
- (45) Giannozzi, P.; Baroni, S.; Bonini, N.; Calandra, M.; Car, R.; Cavazzoni, C.; Ceresoli, D.; Chiarotti, G. L.; Cococcioni, M.; Dabo, I.; et al. QUANTUM ESPRESSO: a modular and open-source software project for quantum simulations of materials. *J. Phys. Condens. Matter* **2009**, *21* (39), 395502.
- (46) Vanderbilt, D. Soft self-consistent pseudopotentials in a generalized eigenvalue formalism. *Phys. Rev. B* **1990**, *41* (11), 7892– 7895.
- (47) Becke, A. D. Density-functional exchange-energy approximation with correct asymptotic behavior. *Phys. Rev. A* **1988**, *38* (6), 3098–3100.
- (48) Lee, C.; Yang, W.; Parr, R. G. Development of the Colle-Salvetti correlation-energy formula into a functional of the electron density. *Phys. Rev. B* **1988**, *37* (2), 785–789.
- (49) Kokalj, A. Computer graphics and graphical user interfaces as tools in simulations of matter at the atomic scale. *Comput. Mater. Sci.* **2003**, *28* (2), 155–168.